biomass

MDPI

Article

Sustainable Valorization of Sugarcane Bagasse Through Lignin Extraction, Bioethanol Production, and a Proof of Concept Lignin Application

Hind Elfahmy [1,*], Doha Elalami [1], Anass Oulkhir [2], Karim Lyamlouli [3] and Zakia El Ahmadi [1]

[1] Department of Process Engineering, Mohammadia School of Engineering (EMI), Mohammed V University, Rabat 10000, Morocco; d.elalami@emi.ac.ma (D.E.)
[2] CNRS, GeoRessources, Université de Lorraine, F-54000 Nancy, France
[3] College of Agriculture and Environmental Sciences (AgBS), Mohammed VI Polytechnic University, Benguerir 43150, Morocco
* Correspondence: elfahmy.hind10@gmail.com

Abstract

Sugarcane bagasse (SCB) represents an abundant lignocellulosic residue with significant potential for integrated biorefinery applications. In this study, an alkaline extraction process was optimized for lignin recovery from SCB using a Box–Behnken Design (BBD) to evaluate the effects of extraction temperature (70–110 °C), NaOH concentration (3–9%, *w*/*v*), solid-to-liquid ratio (1:10–1:50, g mL^{-1}), and extraction time (30–90 min). Total phenolic content (TPC) and pure lignin content (PLC) were employed as response variables to identify optimal extraction conditions. Under the optimized parameters, a lignin yield of 17.7% and a TPC of 52.7 mg GAE g^{-1} were achieved. Structural and thermal characterization by Fourier-transform infrared spectroscopy (FTIR) and thermogravimetric analysis (TGA) confirmed the preservation of characteristic lignin functionalities and adequate thermal stability for downstream applications. To demonstrate its valorization potential, the recovered lignin was successfully incorporated as a partial substitute for petroleum-derived phenol in the formulation of a lignin-based resin, providing a proof of concept for its utilization in sustainable polymeric materials. In parallel, the cellulose-enriched residual solid (RS) obtained after lignin extraction was subjected to fermentation, yielding 10.3 g L^{-1} ethanol. This integrated strategy enabled the sequential production of lignin-derived materials and bioethanol from a single biomass feedstock, maximizing resource utilization while minimizing waste generation. The findings highlight the feasibility of coupling lignin recovery with biofuel production and support the development of SCB-based biorefineries for the generation of renewable chemicals, bio-based materials, and sustainable energy carriers.

Keywords: sugarcane bagasse; lignin extraction; Box–Behnken design; biorefinery; bioethanol; lignin-based resin; biomass valorization; sustainable materials

Check for updates

Academic Editor: Carlo Pastore

Received: 4 June 2026
Revised: 21 July 2026
Accepted: 22 July 2026
Published: 25 July 2026

Copyright: © 2026 by the authors. Licensee MDPI, Basel, Switzerland. This article is an open access article distributed under the terms and conditions of the Creative Commons Attribution (CC BY) license.

1. Introduction

The sugar industry plays a pivotal role in the agricultural and industrial sectors of Morocco, contributing significantly to the national economy. However, this industry also generates considerable amounts of waste, particularly bagasse, the fibrous by-product obtained after the extraction of juice from sugarcane [1,2]. Bagasse represents a rich source of lignocellulosic biomass, which has long been underutilized despite its potential for various high-value applications [3]. The efficient valorization of this biomass could provide

sustainable solutions for waste management while supporting the development of bio-based industries in Morocco.

Lignocellulosic biomass, including bagasse, is primarily composed of cellulose, hemicellulose, and lignin. These three biopolymers are linked together, forming a complex and recalcitrant structure [4,5]. Cellulose and hemicellulose, being carbohydrate-rich, are often targeted for the production of biofuels such as bioethanol. Lignin, on the other hand, is a polyaromatic compound known for its structural rigidity and chemical versatility [6]. Lignin is increasingly recognized for its potential applications due to its high functional group density and ability to bind various contaminants [7]. Despite this potential, the effective valorization of lignin and other components of lignocellulosic biomass depends on efficient fractionation techniques. Alkaline extraction (AE) is one of the most widely used methods for isolating lignin, given the high yield it can achieve [8]. However, achieving high-purity lignin requires the optimization of process parameters such as temperature, reaction time, alkali concentration and solid-to-liquid ratio. Pure lignin after extraction processes can be directly utilized in various industrial applications such as bio-based adhesives, phenolic resins, and biodegradable plastics [9], while the resulting lignin-poor RS is ideally suited for conversion into fermentable sugars and subsequent ethanol production as it contains cellulose and hemicelluloses.

In Morocco, the potential for lignocellulosic biomass valorization, particularly from sugar industry bagasse, remains largely untapped. The sugar industry generates significant amounts of by-products such as bagasse, beet pulp, and molasses, which are mainly used for low-value applications such as energy production and animal feed, despite their high potential for biorefinery applications [10]. With the global push toward sustainable development and renewable energy, there is a growing interest in transforming agricultural by-products into high-value materials and biofuels [11]. The combined valorization of lignin and lignin-poor RS presents a promising pathway for the efficient use of bagasse, addressing both environmental and economic challenges.

Despite the extensive research devoted to SCB valorization, most studies have focused on the production of a single value-added product, such as lignin, bioethanol, biochar, or platform chemicals [12,13]. Lignin, one of the most abundant renewable aromatic polymers in nature, has attracted considerable interest due to its potential applications in the production of bio-based materials, adsorbents, resins, antioxidants, and other value-added chemicals. As a result, numerous studies have focused on the extraction and utilization of lignin from lignocellulosic biomass. However, these processes generate lignin-poor residual biomass fractions that remain insufficiently valorized. Consequently, the integrated utilization of both lignin and the RS within a comprehensive biorefinery framework remains insufficiently explored [14]. Furthermore, although AE has been widely recognized as an effective method for lignin recovery, limited studies have simultaneously optimized lignin extraction conditions and investigated the subsequent valorization of both the recovered lignin and the lignin-depleted residual biomass. Therefore, the development of an integrated strategy combining optimized lignin extraction, lignin-based material production, and bioethanol generation from the residual fraction represents a promising approach to maximize biomass utilization, improve process sustainability, and enhance the overall efficiency of lignocellulosic biorefineries [15].

In this context, the present study proposes an integrated biorefinery approach for the comprehensive valorization of SCB. The objectives were (i) to optimize alkaline lignin extraction using a Box–Behnken experimental design to maximize lignin purity, (ii) to evaluate the conversion of the lignin-poor RS into bioethanol through acid hydrolysis and fermentation, and (iii) to investigate the utilization of the recovered lignin as a partial phenolic substitute in resin formulation. By combining these valorization pathways within

a single process, this work aims to enhance the utilization efficiency of SCB and contribute to the development of sustainable lignocellulosic biorefineries.

2. Materials and Methods

2.1. SCB Preparation and Its Composition Analysis

SCB was collected from the sugar industry (COSUMAR). The raw material was manually cut into small pieces, oven-dried at 105 °C for 20 h, then ground and sieved to obtain particles smaller than 0.5 mm before being subjected to the AE process. The drying temperature (105 °C) was selected to ensure complete moisture removal and accurate determination of biomass dry weight. According to previous studies, drying at this temperature primarily removes residual moisture and does not significantly affect the structural integrity of lignin, cellulose, and hemicellulose over the duration employed in this study [16].

The chemical composition of SCB was determined using standard analytical methods. The procedures followed widely accepted protocols commonly used for lignocellulosic biomass characterization, with adaptations from established methods such as those developed by the National Renewable Energy Laboratory (NREL) where appropriate. The proximate analysis of SCB was conducted according to ASTM standard methods to determine its moisture and ash contents [17]. Klason lignin content was determined using a two-step acid hydrolysis method, where lignin was quantified as the acid-insoluble residue [18]. Acid Detergent Fiber (ADF) analysis was conducted to estimate cellulose and lignin fractions, while hemicellulose content was calculated by difference [19]. Additionally, acid hydrolysis using 0.05 N HCl was carried out to facilitate the fractionation of structural carbohydrates.

2.2. Experimental Design for the AE Process

The previously prepared SCB was used as the feedstock for the AE experiments. For the solid-to-liquid ratios investigated in the BBD (1:10–1:50, *w*/*v*), the biomass amount ranged from 2 to 5 g, while the corresponding volume of NaOH solution ranged from 20 to 100 mL with concentrations varying from 3 to 9 wt.%, according to the experimental design. The mixture was then heated at various temperatures between 70 and 110 °C for extraction times ranging from 30 to 90 min. Following the extraction step, the RS was separated from the black liquor by filtration. The residue was washed with distilled water three times and then dried in an oven at 50 °C for 48 h. The black liquor was treated with H_2SO_4 at 2.5 M to precipitate lignin. The solution was centrifuged at 6000 rpm for 15 min and washed three times with distilled water. Finally, the extracted lignin (E-Lign) was dried in an oven at 50 °C for 48 h. The ranges of the independent variables used in the BBD were selected based on preliminary experiments and previously reported studies on AE of lignocellulosic biomass [7,8,13], ensuring effective lignin solubilization while avoiding excessive degradation of the biomass structure.

The Response Surface Methodology (RSM) allows the optimization of the conditions of lignin extraction from SCB with minimal number of experiments. A BBD with four variables and three levels (−1, 0, +1) shown in Table 1 was applied to study the effect of the reaction time (30–60–90 min; t), extraction temperature (70–90–110 °C; *T*), NaOH concentration in the extraction solution (3–6–9% in volume; *C*), and solid-to-liquid ratio (1/10–1/16.8–1/50, *w*/*v*; *R*) on the lignin yield and the TPC. The R is expressed as a coded variable in the BBD, corresponding to the actual experimental values of 1:10, 1:16.8, and 1:50 (*w*/*v*), respectively. Table 2 indicates that the design was implemented for a total of 27 lignin extraction experiments with three replications. The Design Expert software (Version 2011, USA) was used for the statistical analysis of the data and for optimizing the four factors to determine the optimal extraction parameters.

Table 1. Experimental ranges and coded levels of the independent variables considered in the BBD for optimization of lignin extraction from SCB.

Independent Variables	Units	Factors	Variable Ranges		
			−1	**0**	**+1**
NaOH Concentration	%	C	3	6	9
Temperature	°C	T	70	90	110
S/L Ratio	*w*/*v*	R	1/10	1/16.8	1/50
Time	min	t	30	60	90

Table 2. BBD of coded independent variables.

Experiment	T (°C)	R	C (%)	t (min)
1	70	1/50	6	60
2	110	1/50	6	60
3	70	1/10	6	60
4	110	1/10	6	60
5	90	1/16.8	3	30
6	90	1/16.8	9	30
7	90	1/16.8	3	90
8	90	1/16.8	9	90
9	70	1/16.8	6	30
10	110	1/16.8	6	30
11	70	1/16.8	6	90
12	110	1/16.8	6	90
13	90	1/50	3	60
14	90	1/10	3	60
15	90	1/50	9	60
16	90	1/10	9	60
17	70	1/16.8	3	60
18	110	1/16.8	3	60
19	70	1/16.8	9	60
20	110	1/16.8	9	60
21	90	1/50	6	30
22	90	1/10	6	30
23	90	1/50	6	90
24	90	1/10	6	90
25	90	1/16.8	6	60
26	90	1/16.8	6	60
27	90	1/16.8	6	60

The TPC (Y1) and the yield of PLC (Y2) were analyzed using the multiple regression model. The statistical analysis of the experimental data was carried out using Design Expert software. Analysis of variance (ANOVA) was employed to assess the significance and adequacy of the developed model. The significance of each factor and their interactions was evaluated based on *p*-values (with a significance level of 0.05). In addition, the coefficient of determination (R^2) and the adjusted R^2 were examined to evaluate the model's accuracy and predictive capability.

2.3. Analysis of Lignin Extracts

2.3.1. Determination of TPC

The protocol used for the determination of *TPC* is based on that described in a previous study [20]. In a micro-plate a volume of 20 µL of each extract was added, with a mixture of 100 µL of Folin–Ciocalteu reagent diluted 10-fold, and 80 µL of a 7.5% sodium carbonate solution. The micro-plate was incubated for 30 min. Absorbance was read at 735 nm using UV–Vis spectrophotometer (FLUOstar Omega, BMG LABTECH, Ortenberg, Germany). A calibration curve was run in parallel under the same operating conditions, using gallic acid at different concentrations.

2.3.2. Purity Lignin Analysis

The lignin purity was determined by a two-stage acid hydrolysis method as previously described [18]. A sample of 80 mg of lignin was gradually added to 0.8 mL of 72% H_2SO_4 and incubated in a water bath at 30 °C for 1 h. Then, 23.8 mL of distilled water was added to dilute the mixture. After being diluted, the mixture was heated under reflux until the boiling temperature reached 120 ° for 1 h, and the insoluble residue was left to settle. Filtration was carried out in a weighted sintered crucible, and washed with 500 mL of distilled water preheated to approximately 80 °C. After washing, it was dried in an oven at 105 °C for 12 h. The residue obtained is Klason lignin and was then weighed (Equation (1)).

$$\text{Purity} = \frac{\text{weight of Klason Lignin (g)}}{\text{weight of extracted matter (g)}} \quad (1)$$

The extraction yield was expressed as a percentage of the initial dry biomass weight (Equation (2)). This calculated yield represents the E-Lign, which may include impurities. Then, the second response represents the PLC after each trial (Equation (3)).

$$\text{Extraction Yield (\%)} = \frac{\text{weight of extracted matter (g)}}{\text{Initial Dry Massof Bagasse (g)}} \times 100 \quad (2)$$

$$\text{Y2(\%)} = \text{Extraction Yield(\%)} \times \text{Purity} \quad (3)$$

2.3.3. Characterization of Lignin Extracts Prepared Under Optimal Conditions

Structural and thermal characterization of the E-Lign and RS was performed by FTIR, and TGA. FT-IR measurements were taken using an FT-IR Nicolet 6700 (Thermos, Schaumburg, IL, USA). Each scan recorded 50 scans, in the range from 500 to 4000 cm^{-1} with a resolution of 4 cm^{-1} according to the method described in [21]. TGA was conducted using a thermogravimetric analyzer instrument, covering a temperature range of 100 °C to 900 °C, with a heating rate of 10 °C min^{-1} according to the method described in [22].

2.4. Bioconversion of RS into Ethanol

The RS obtained after AE under optimized conditions and the Untreated Sugarcane Bagasse (UT-SCB) were subjected to acid hydrolysis and subsequent fermentation for ethanol production. The hydrolysis step was carried out using the lignin-free acidic filtrate

(LFAF) recovered after lignin precipitation from black liquor at pH 2, thereby promoting biomass valorization while minimizing the use of additional chemical reagents. In this process, acidification of the black liquor to pH 2 was specifically performed to precipitate lignin, allowing its separation from the liquid phase. The resulting LFAF mainly contains inorganic salts, residual soluble sugars, and low-molecular-weight organic compounds. This stream was directly reused as the hydrolysis solution for the RS, which was the actual substrate for hydrolysis. The hydrolysis was performed at a solid-to-liquid ratio of 1:10 (w/v), a temperature of 120 °C, and a residence time of 2 h under controlled conditions. Following hydrolysis, the resulting hydrolysate was cooled and neutralized with NaOH to pH 5.5 ± 0.1. Fermentation was carried out using *Saccharomyces cerevisiae* in 250 mL Erlenmeyer flasks with a working volume of 100 mL. A 5% (v/v) inoculum of actively growing yeast culture was added. The process was conducted under anaerobic conditions achieved by sealing the flasks, at 30 °C and 140 rpm for 72 h, during which fermentable sugars were converted into ethanol [23].

The fermentation performances of RS and UT-SCB were compared based on ethanol production. Following fermentation, the broth was centrifuged to remove residual yeast cells and fine suspended particles. The resulting supernatant was filtered through a 0.2 µm membrane filter prior to Gas Chromatography–Mass Spectrometry (GC–MS) analysis. The clarified filtrate was analyzed using a Shimadzu GCMS-TQ8040 NX system equipped with an Rxi-5Sil MS capillary column (30 m × 0.25 mm × 0.25 µm). Analyses were performed in split injection mode (split ratio 5:1) using helium as the carrier gas. The oven temperature was initially maintained at 50 °C for 2 min, increased at 5.5 °C min^{-1} to 300 °C, and held for 3 min. For ethanol quantification, an external calibration curve was established using six ethanol standard solutions covering the concentration range of 0.25–12.0 g L^{-1} (Figure 1). All standards were analyzed using the same Shimadzu GC–MS system under identical chromatographic conditions as those employed for the fermentation samples. Linear regression of peak area versus ethanol concentration produced the following calibration equation:

$$y = 3E + 06x + 783{,}218 \quad (4)$$

where y represents the GC–MS peak area and x the ethanol concentration (g L^{-1}).

2.5. Preparation of Resin Based on E-Lign

The resin was synthesized according to a previously reported procedure with slight modifications [24]. In a typical experiment, 0.5 g of extracted alkali lignin and 0.5 g of sodium hydroxide were dissolved in 10 mL of distilled water under mechanical stirring. Subsequently, 10 mL of a glutaraldehyde/glyoxal solution (1:1, v/v) was introduced as the crosslinking agent. The reaction mixture was maintained at 80 °C for 45 min under continuous stirring. Afterward, the system was cooled to 40 °C to terminate the reaction. The resulting resin was then cured at 110 °C for 3 h in an oven. The prepared resin was further characterized by FTIR spectroscopy to identify the functional groups and confirm the formation of the cross-linked structure. In addition, solubility tests were performed in 0.1 M and 0.05 M NaOH solutions, ethanol, and distilled water to evaluate the chemical stability of the synthesized resin.

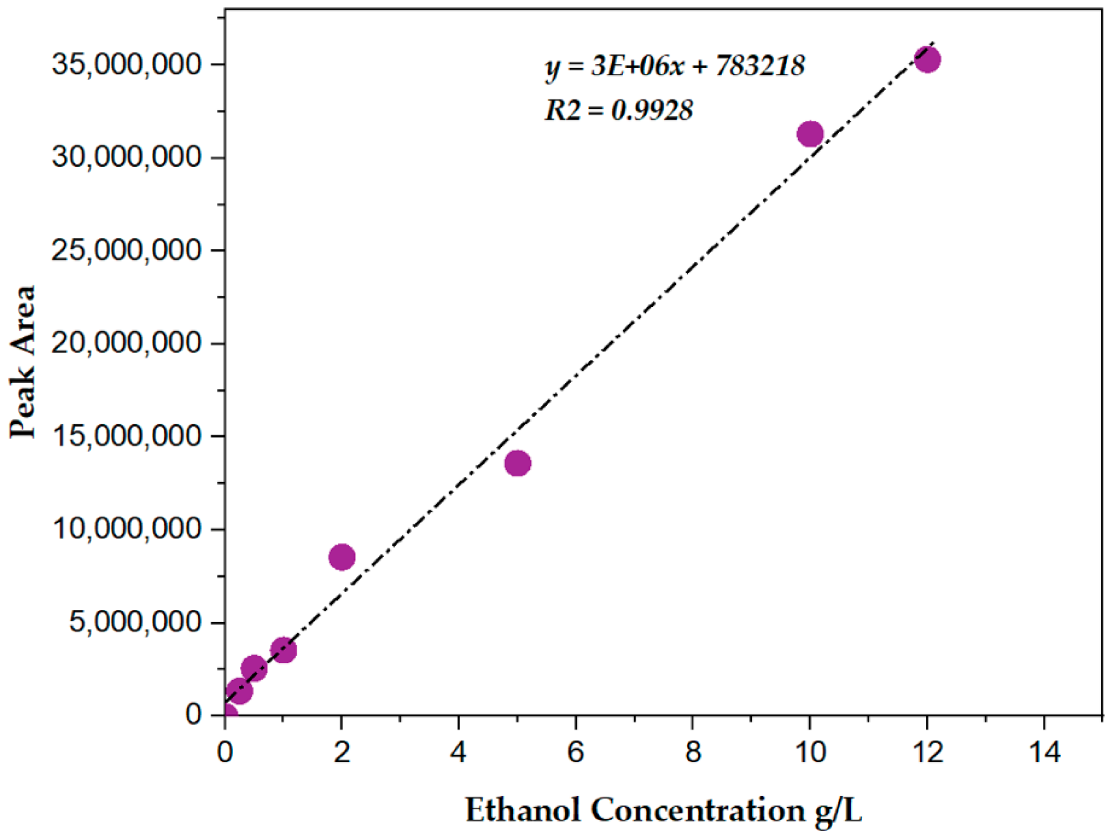


Figure 1. External calibration curve used for ethanol quantification by GC–MS. Purple circles represent the experimental calibration data, while the dashed line represents the linear regression fit.

3. Results

3.1. Composition of SCB

The moisture content of SCB was 8.3 ± 0.1%, corresponding to a dry matter content of 91.7 ± 0.1%, indicating a relatively low water content and a high proportion of solid material suitable for subsequent extraction and biorefinery processes. The ash content was 3.7 ± 0.1%, which falls within the typical range reported in the literature (1–4%) [25]. Lignin content was 22.6 ± 0.3% (dry basis), consistent with previously reported values [26]. Cellulose accounted for 34.8 ± 0.5% of the dry weight, confirming SCB as a rich source of glucose polymers suitable for bioethanol production. Hemicellulose represented 36.6 ± 1.2% of the dry matter, indicating a substantial fraction of pentose sugars that can be further valorized through bioconversion processes [27]. Although cellulose is often reported as the predominant carbohydrate fraction in SCB, the relative proportions of cellulose and hemicellulose may vary depending on cultivar, geographical origin, growth conditions, and analytical methodology. In addition, the analytical procedures employed in the present study, where carbohydrate fractions were estimated using a combination of ADF measurements and difference calculations, may contribute to slight variations in the distribution of these fractions. Therefore, the observed composition remains within the range commonly reported for lignocellulosic biomass and is consistent with the natural variability reported for SCB [28]. These compositional characteristics highlight the potential of SCB as a versatile feedstock for both bioethanol production and the development of lignin-based value-added materials.

3.2. Effect of Operational Variables on the Extraction of the Lignin

The overall extraction yield, explicitly reported in Table 3, ranged from 16.2 to 23.3%, while TPC values varied from 32.2 to 52.7 mg GAE g^{-1} and PLC values from 9.8 to 17.9%, indicating the effectiveness of the AE process under the investigated conditions. From a

comparative perspective, the extraction yields achieved in the present study (16.2–23.3%) surpassed those reported for alkaline pulping under relatively mild processing conditions. In the latter studies, lignin yields of 13.0% and 7.2% were obtained following hot-water pretreatment combined with NaOH pulping under different operational conditions, reflecting the influence of process severity on lignin recovery [29,30]. The observed differences may be attributed to variations in process severity and extraction conditions. Among the investigated factors, temperature and solid-to-liquid ratio exerted the most pronounced influence on both responses. The highest TPC value (52.7 mg GAE g^{-1}) was obtained in Experiment 18; this observation is consistent with the positive effect of elevated temperature on phenolic compound release. Higher temperatures generally enhance lignin dissolution by promoting the cleavage of ether linkages and improving mass transfer, as reported in the literature [31,32]. Experiment 16 exhibited the highest extraction yield (23.3%) and PLC (17.9%), suggesting the strong influence of the solid-to-liquid ratio on both recovery efficiency and effective lignin content. Under comparable operating conditions, increasing the extraction time from 30 min (Experiment 6) to 90 min (Experiment 7) resulted in an increase in TPC from 47.1 to 49.2 mg GAE g^{-1} and in PLC from 14.3 to 16.8%, indicating improved lignin solubilization with prolonged treatment. In contrast, variations in NaOH concentration produced less pronounced changes in both responses, suggesting that alkaline conditions were already sufficient within the investigated range. These findings are consistent with previous studies highlighting the critical role of process parameters in AE.

The evaluation of AE performance in this study was based on three complementary indicators: (i) the overall extraction yield, representing the total mass of lignin-rich fraction recovered from the dry biomass; (ii) the lignin purity, reflecting the quality of the extracted fraction; and (iii) the PLC, representing the effective lignin content recovered from the extracted fraction. These three parameters were selected to provide a comprehensive evaluation of the extraction process. While extraction yield reflects the total amount of recovered material, it does not distinguish lignin from co-extracted impurities. Conversely, lignin purity alone does not account for the total recovery efficiency. Therefore, PLC was introduced as an integrated indicator combining both yield and purity, enabling a more realistic assessment of the actual lignin recovery from SCB. It is important to note that most published studies on lignin valorization from lignocellulosic biomass primarily report lignin removal efficiency or delignification performance rather than extraction yield. Therefore, the literature comparisons are often based on lignin removal or fractionation efficiency as complementary indicators. In this context, the present results are consistent with AE trends, where yield increases with process severity and pretreatment intensity. Therefore, the literature comparisons are often based on lignin removal or fractionation efficiency as complementary indicators. In this context, the present results are consistent with the general trends reported for AE, where lignin recovery increases with process severity and pretreatment intensity. High lignin recovery (72.8%) has been reported using 6% NaOH at 90 °C for 1 h with a liquid-to-solid ratio of 15 [33]. Alternative pretreatment strategies have also been investigated, including deep eutectic solvent treatment, which achieved 55% lignin removal [34], and organosolv fractionation, which produced lignin with a purity of approximately 80% under relatively mild operating conditions [35]. A lignin removal efficiency of 86.7% has also been reported for alkaline-pretreated SCB subjected to subsequent deep eutectic solvent treatment [36].

Table 3. Results obtained under different AE conditions as determined by the BBD.

Experiment	Y1 (mgGAE/g)	Extraction Yield (%)	Purity (%)	Y2 (%)
1	32.1 ± 0.2	16.7 ± 0.4	58.8 ± 0.3	9.8 ± 0.2
2	37.1 ± 0.2	18.6 ± 0.6	63.5 ± 0.2	11.8 ± 0.4
3	43.2 ± 0.3	19.3 ± 1.2	67.9 ± 1.0	13.1 ± 1.1
4	47.4 ± 0.4	20.3 ± 1.1	86.3 ± 1.0	17.5 ± 1.3
5	41.5 ± 0.3	19.2 ± 1.2	78.8 ± 0.9	15.1 ± 1.1
6	47.1 ± 0.2	18.1 ± 0.7	79.1 ± 0.9	14.3 ± 0.8
7	49.2 ± 0.1	20.5 ± 0.8	82.1 ± 0.3	16.8 ± 0.7
8	48.3 ± 0.4	19.5 ± 1.2	81.0 ± 1.1	15.7 ± 1.2
9	36.8 ± 0.1	18.5 ± 1.0	65.7 ± 0.1	12.1 ± 0.7
10	42.1 ± 0.3	18.5 ± 0.7	79.2 ± 0.6	14.6 ± 0.5
11	38.4 ± 0.2	17.8 ± 0.6	69.3 ± 0.4	12.3 ± 0.4
12	47.2 ± 0.3	20.2 ± 0.8	78.3 ± 0.5	15.8 ± 0.6
13	32.3 ± 0.1	16.3 ± 0.2	61.2 ± 0.1	9.9 ± 0.1
14	46.4 ± 0.3	20.1 ± 1.5	80.9 ± 0.4	16.2 ± 1.2
15	33.9 ± 0.1	16.2 ± 0.3	76.3 ± 0.2	12.3 ± 0.3
16	49.3 ± 0.4	23.3 ± 1.4	84.2 ± 0.6	17.9 ± 1.2
17	39.4 ± 0.4	16.3 ± 0.8	71.8 ± 0.5	11.7 ± 0.6
18	52.7 ± 0.2	18.2 ± 0.5	81.2 ± 0.4	14.7 ± 0.4
19	41.8 ± 0.3	18.6 ± 0.9	73.7 ± 1.0	13.7 ± 0.7
20	51.4 ± 0.3	21.3 ± 0.4	82.1 ± 0.7	17.4 ± 0.4
21	33.1 ± 0.2	16.6 ± 0.5	62.4 ± 0.3	10.3 ± 0.3
22	46.3 ± 0.3	17.2 ± 0.9	79.8 ± 0.9	13.7 ± 0.7
23	41.0 ± 0.1	19.3 ± 0.5	75.0 ± 0.2	14.4 ± 0.4
24	47.6 ± 0.1	20.7 ± 1.2	85.6 ± 1.1	17.7 ± 1.1
25	38.4 ± 0.4	19.2 ± 0.5	76.1 ± 0.4	14.6 ± 0.4
26	41.8 ± 0.4	18.7 ± 0.7	78.5 ± 0.7	14.6 ± 0.5
27	40.2 ± 0.2	18.5 ± 0.8	79.3 ± 0.4	14.6 ± 0.7

3.3. Validation of Models

The experimental data were fitted to a second-order polynomial model, and the adequacy of the model was evaluated using analysis of variance (ANOVA). As presented in Table 4, T and R were identified as the most influential factors affecting both Y1 and Y2, with highly significant *p*-values ($p < 0.01$). In contrast, C showed no significant linear effect on either response within the investigated range ($p > 0.05$). t exhibited a significant positive influence on both responses, although its effect was less pronounced than those of temperature and S/L ratio. Regarding the quadratic terms, only C^2 significantly affected Y1 ($p = 0.003$), suggesting the existence of a nonlinear relationship between alkali concentration and phenolic recovery. Furthermore, none of the interaction terms were statistically significant ($p > 0.05$), indicating that the effects of the investigated factors were predominantly independent. Furthermore, the adequacy of the models was evaluated using the correlation coefficient (R^2) and the adjusted correlation coefficient (R^2 adj). For the TPC response, the regression model showed R^2 = 90.5% and R^2 adj = 78.4%, while for the PLC response, the

model yielded R^2 = 88.2% and R^2 adj = 74.5%, reflecting a good agreement between the experimental and predicted values. Although the adjusted coefficients of determination were lower than the corresponding R^2 values, they remained sufficiently high, indicating that a substantial proportion of the response variability was explained by the selected model terms. This suggests that the developed models retained satisfactory predictive capability while accounting for the number of variables included in the regression. In addition, the adequacy of the models was further confirmed by the statistical significance of the regression ($p < 0.05$), demonstrating that the observed relationships between the process variables and the responses were unlikely to have occurred by chance. Collectively, these statistical indicators support the reliability and suitability of the developed models for describing and predicting the behavior of the system within the investigated experimental domain [37].

Table 4. ANOVA results for the regression equations describing the effects of process variables on Y1 and Y2.

	Y1		Y2	
	Coef.	***p*-Value**	**Coef.**	***p*-Value**
Constant	57.3	0.000	−8.9	0.000
T	−0.382	0.001	0.386	0.001
R	402	0.000	63.6	0.000
C	−6.00	0.978	−0.67	0.118
t	−0.293	0.033	−0.020	0.010
T × T	0.00270	0.389	−0.00218	0.114
R × R	−924	0.246	−534	0.121
C × C	0.499	0.003	0.0604	0.310
t × t	0.00220	0.128	0.000194	0.739
T × R	−0.35	0.844	0.759	0.325
T × C	−0.0004	0.988	0.00292	0.773
T × t	0.00166	0.489	0.000408	0.686
R × C	−3.7	0.758	−1.52	0.763
R × t	−1.38	0.258	−0.025	0.960
C × t	0.0044	0.779	−0.00061	0.928

To further assess the predictive performance of the developed models, the predicted values were compared with the experimental data (Figure 2). The results show that the data points are closely distributed along the diagonal line for both responses, indicating a strong agreement between predicted and actual values. This confirms the good accuracy and reliability of the developed models. The relatively low dispersion of the data points around the regression line suggests minimal prediction error and the absence of significant bias in the model. These observations are consistent with the high R^2 values obtained, further validating the suitability of the models for prediction and optimization purposes. The experimental data were fitted to a second-order polynomial model.

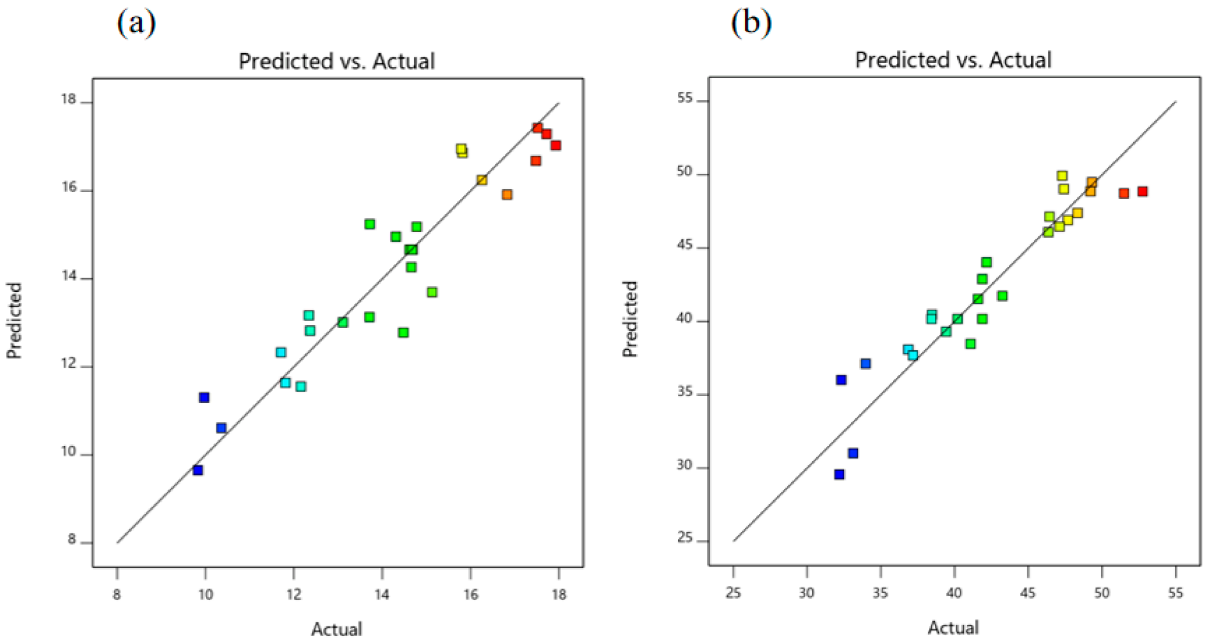


Figure 2. Predicted versus actual values obtained from the developed models: (**a**) TCP and (**b**) PLC. The colored squares represent the experimental data points used for model validation.

3.4. RSM for Process Optimization

Figure 2 presents the three-dimensional response surface plots illustrating the interaction effects of the studied variables on TPC and PLC. For both responses, the surface plots (Figure 3a–c for TPC and Figure 3d–f for PLC) consistently indicate that temperature and solid-to-liquid (S/L) ratio are the most influential factors, exhibiting a strong positive effect on extraction efficiency. In both cases, the simultaneous increase in these two variables leads to higher response values, as reflected by the pronounced curvature of the surfaces, confirming a synergistic interaction between them. In contrast, NaOH concentration and extraction time show relatively weaker effects, as evidenced by flatter surface profiles across the studied range. Moreover, the curvature observed along the temperature axis suggests significant quadratic effects, highlighting its dominant role within the experimental domain. Overall, similar trends are observed for both TPC and PLC, and the results are consistent with the regression analysis and ANOVA outputs, confirming the adequacy of the quadratic models.

Compared with previous studies [38,39], in which the solid-to-liquid ratio was maintained at a fixed value, the present study incorporated this parameter into the optimization design. The results clearly demonstrated that the solid-to-liquid ratio is a key parameter governing extraction efficiency by improving mass transfer and reagent accessibility to the biomass structure. Importantly, beyond its impact on lignin extraction performance, the solid-to-liquid ratio also influences the physicochemical characteristics of the resulting RS. Appropriate operating conditions promote selective lignin removal while preserving the carbohydrate-rich fraction of the biomass. This is particularly advantageous in an integrated biorefinery approach, as it enhances the susceptibility of the residual substrate to subsequent hydrolysis and fermentation, thereby improving the efficiency of bioethanol production.

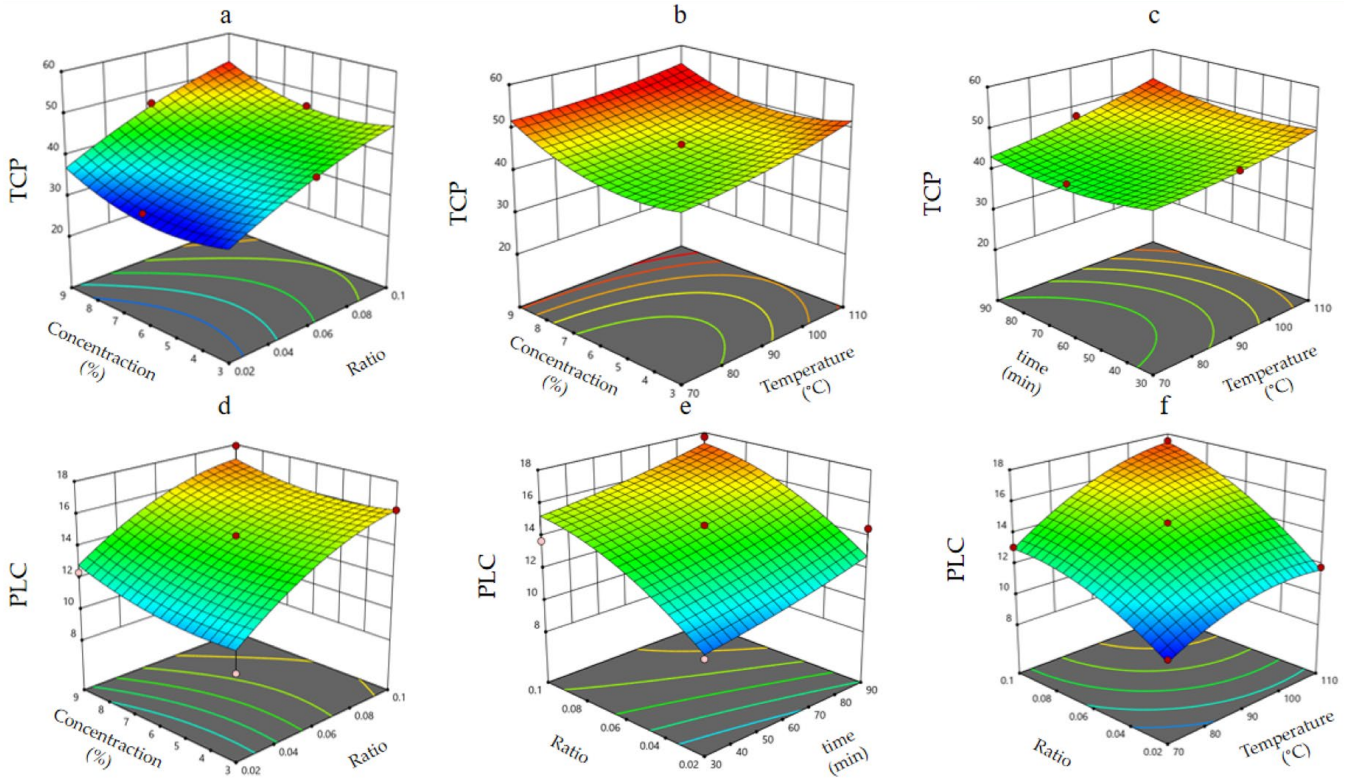


Figure 3. Three-dimensional response surface plots generated from the RSM models for TPC and PLC. The variables studied are temperature (T, °C), NaOH concentration (C, %), extraction time (t, min), and solid-to-liquid ratio (R, S/L). The response surfaces illustrate the interaction effects between the variables and their influence on TPC and PLC. Panels (**a**–**c**) represent the effects of the operating variables on TPC, while panels (**d**–**f**) show their effects on PLC.

3.5. Optimal Conditions for Lignin Extraction

Numerical optimization of the lignin extraction process from SCB was performed using Design-Expert software based on the developed RSM to determine the optimum extraction conditions. As shown in Figure 4, the optimization predicted a PLC of 17.7% and a TPC of 52.7 mg GAE/g under optimal conditions of 108.6 °C, a solid-to-liquid ratio of 1/10.5, a NaOH concentration of 8.9%, and a reaction time of 43.9 min. It should be noted that several optimal conditions were located at the boundaries of the experimental ranges, specifically temperature, solid-to-liquid ratio and NaOH concentration. Despite being located at the experimental limits, validation experiments conducted under these conditions produced consistent and reproducible results, confirming the robustness and reliability of the optimization process. Therefore, the identified optimum conditions represent the best achievable performance within the experimental domain investigated in the study. The optimized NaOH concentration (8.9 wt.%) was predicted using the desirability function, which simultaneously optimizes multiple responses by combining them into a single objective function. Although NaOH concentration was not identified as a statistically significant factor in the ANOVA, it was included in the numerical optimization performed using the predictive RSM model. Consequently, the predicted optimum represents the maximum global desirability within the investigated experimental domain and should be interpreted as the mathematical optimum predicted by the model rather than evidence that 8.9 wt.% is statistically superior to lower NaOH concentrations. From a practical standpoint, however, lower NaOH concentrations may constitute more suitable operating conditions whenever comparable extraction performance is achieved, owing to reduced chemical consumption, lower operating costs, and a lower environmental impact.

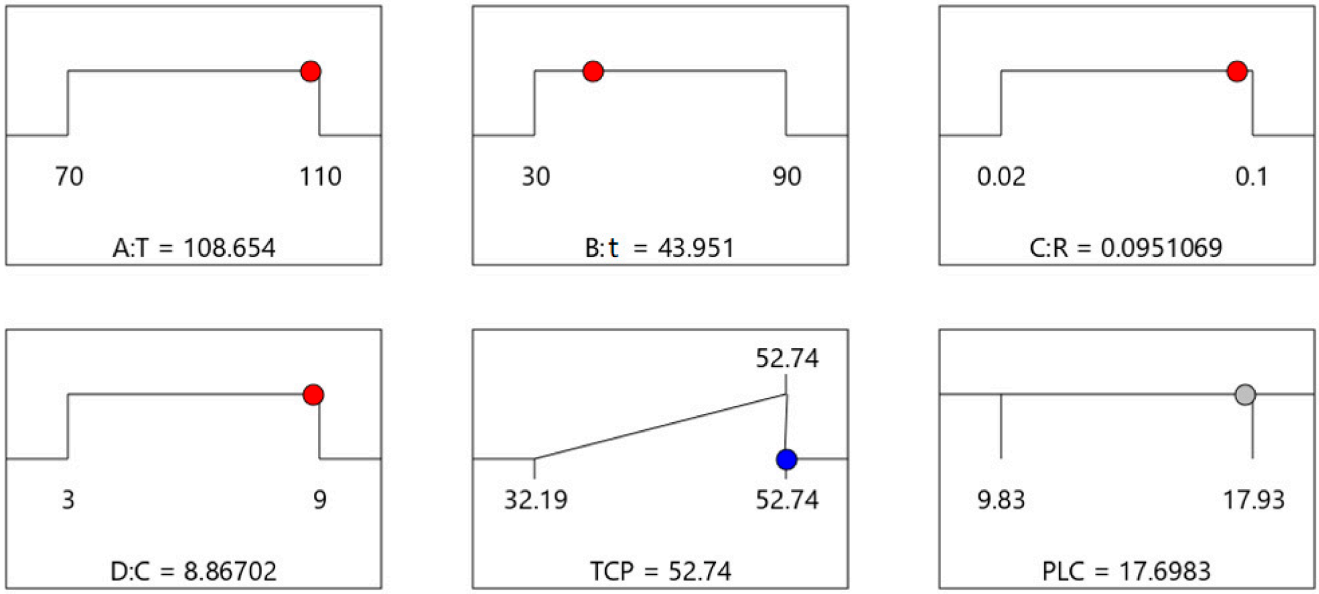


Figure 4. Optimal extraction conditions determined by BBD. Red dots indicate the optimal levels of the independent variables (A–D), while the blue and grey dots represent the predicted values of Y1 (PLC) and Y2 (TPC), respectively, under the optimal conditions.

3.6. Characterization of E-Lign and RS Under Optimum Conditions

For structural confirmation of E-Lign, TGA and FTIR analysis were performed. The FTIR spectra are presented in Figure 5a. The presence of characteristic peaks in FTIR spectra indicates the presence of lignin in the sample, such as the peak at ~3284 cm^{-1} which corresponds to O–H stretching vibrations, indicating the presence of phenolic and alcoholic hydroxyl groups [40]. Peaks at ~2920 cm^{-1} represent C–H stretching in methyl and methylene groups, suggesting aliphatic side chains within the lignin structure. The aromatic nature of lignin is confirmed by the peaks at ~1623 cm^{-1} and ~1520 cm^{-1}, attributed to C=C stretching vibrations in the aromatic rings, indicative of guaiacyl, syringyl, and p-hydroxyphenyl units [41]. Additionally, the peak at ~1458 cm^{-1} reflects aromatic ring vibrations or methoxy group contributions, while the peak at ~1324 cm^{-1} corresponds to guaiacyl ring breathing and C–O stretching. Peaks at ~1024 cm^{-1} are associated with C–O stretching in alcohols [42]. These observations confirm the successful isolation of a lignin-rich fraction with high structural integrity under the optimized extraction conditions [43,44]. The data from the FTIR spectroscopy show agreement and similarity with the recently published results for lignin [45,46].

In contrast, the FTIR spectrum of the RS reveals notable differences, reflecting its altered composition post-lignin extraction. The broad band around 3500–3300 cm^{-1}, representing O–H stretching vibrations, is still present but less intense, indicating the dominance of hydroxyl groups primarily from cellulose. The peaks at 2889 cm^{-1} are reduced in intensity, reflecting the removal of lignin's aliphatic chains. The significant weakening of the aromatic peaks in the range 1636 cm^{-1} and 1424 cm^{-1} confirms the depletion of lignin content in the solid residue. A significant feature in the solid residue spectrum is the sharp band at 1021 cm^{-1}, corresponding to C–O stretching vibrations, which is primarily attributed to cellulose [47].

The curve of the TGA of lignin as a function of the temperature at a heating rate of 10 °C/min is given in Figure 5b. The TGA curve of the E-Lign aligns with typical thermal degradation profiles reported in prior studies [48,49]. Initially, a weight loss of approximately 10% occurs below 200 °C, which is attributed to the evaporation of physically adsorbed water and low-molecular-weight volatiles. Previous studies have reported that

lignin generally contains hydrophilic functional groups such as hydroxyls, which are responsible for its moisture retention [50]. The most significant weight loss, approximately 50%, is observed between 200 °C and 500 °C, corresponding to the decomposition of lignin's complex polymeric structure. During this stage, degradation involves the cleavage of β-O-4 linkages, as well as the breakdown of aliphatic chains and phenolic groups. Lignin degradation in this range releases volatile compounds like carbon monoxide and carbon dioxide. Beyond 500 °C, the weight loss slows significantly, leaving approximately 20% of the weight as a carbonaceous residue (char), which is consistent with lignin's aromatic and cross-linked nature [51]. In contrast, between 200 °C and 400 °C, the RS experiences the most significant weight loss. In the range of 400 °C to 600 °C, it exhibits minimal degradation. Beyond 600 °C, it was nearly completely degraded at these temperatures, highlighting the low content of lignin and its dominance of polysaccharides [52].

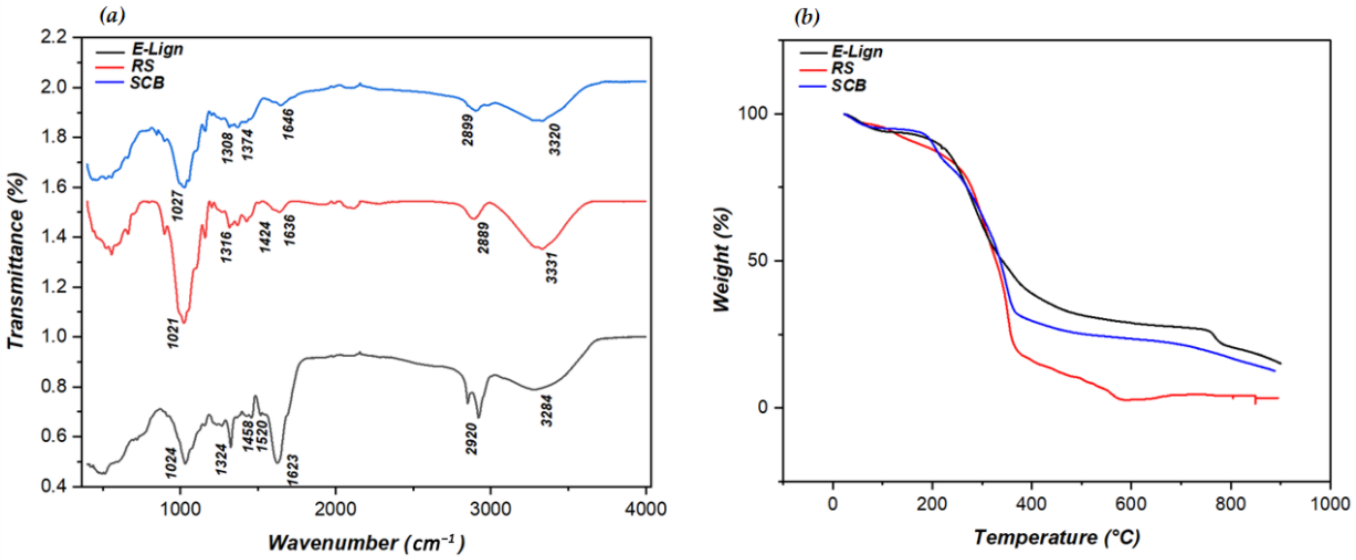


Figure 5. (**a**) FTIR spectra of E-Lign, RS, and SCB samples. Characteristic absorption bands are labeled with their corresponding wavenumbers (cm^{-1}). The black line represents E-Lign, the red line represents RS, and the blue line represents SCB. (**b**) TGA profiles of E-Lign, RS, and SCB samples obtained under the optimal AE conditions.

3.7. Ethanol Production from RS and Fermentation Performance

The GC–MS analysis of the fermentation broth obtained from RS (Figure 6b) identified ethanol as the predominant compound, accounting for 71.3 ± 2.3% of the total detected peak area, with a spectral similarity score of 95%, confirming its reliable identification. L-Alanine ethylamide represented 22.4 ± 1.8% of the detected compounds, suggesting the occurrence of biochemical transformations during fermentation, as *Saccharomyces cerevisiae* is known to synthesize L-alanine through transamination reactions associated with glycolytic metabolism [53]. Among the detected secondary metabolites, 3-methyl-1-butanol represented 4.1 ± 0.9% of the total peak area, while other minor volatile compounds, including ethyl acetate, isopropyl acetate, 2-furanmethanol, 3-methyl-1-butyl acetate, toluene, and 2-pentanone, were detected at lower abundances but contributed to the overall secondary metabolite profile, further confirming the formation of fermentation-derived by-products while ethanol remained the dominant compound [54]. In comparison, fermentation of UT-SCB (Figure 6a) also resulted in ethanol production as the major detected compound, although at a lower relative abundance (56.2 ± 1.1%). Compared with RS, UT-SCB fermentation exhibited higher proportions of L-alanine ethylamide (27.8 ± 2.5%) and 3-methyl-1-butanol (9.9 ± 1.2%), indicating differences in the distribution of fermentation-derived metabolites. The remaining volatile profile was comparable to that observed for RS, with

the presence of similar minor compounds, suggesting comparable secondary metabolite formation pathways during fermentation.

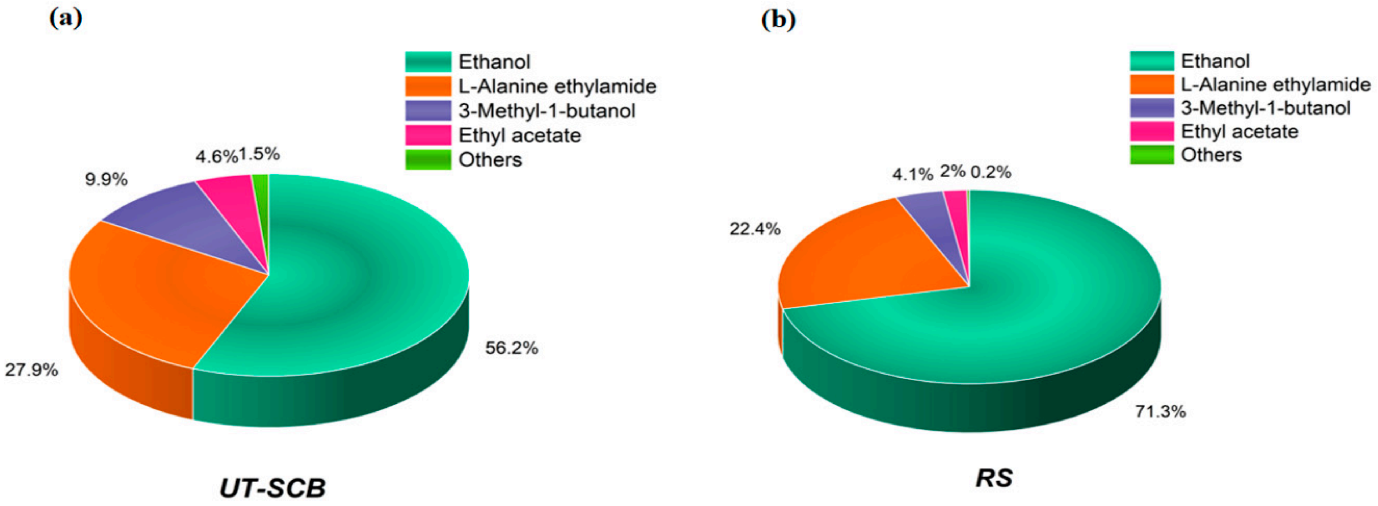


Figure 6. GC–MS analysis of the fermentation products obtained from UT-SCB and RS: (**a**) Relative distribution of the major volatile compounds identified in the fermentation broth of UT-SCB. (**b**) Relative distribution of the major volatile compounds identified in the fermentation broth of RS.

The ethanol concentration, quantified using the instrument-specific GC–MS calibration curve, was 5.6 g L^{-1} for UT-SCB, whereas fermentation of the RS produced 10.3 g L^{-1}, corresponding to an approximately 84.6% increase in ethanol concentration under identical fermentation conditions. This substantial improvement suggests that AE effectively removed a significant fraction of lignin while preserving the carbohydrate-rich fraction, thereby enhancing cellulose accessibility and increasing the availability of fermentable sugars for yeast metabolism. Consequently, the lignin-poor residue generated after AE could be successfully converted into bioethanol, demonstrating the feasibility of integrating lignin recovery with downstream bioethanol production. Furthermore, the reuse of the LFAF for the hydrolysis of both untreated and pretreated biomasses contributes to improved process integration by reducing reagent consumption and promoting a more efficient utilization of process streams within the proposed integrated biorefinery approach. Collectively, these findings demonstrate the potential of a sequential biomass valorization strategy in which both lignin and carbohydrate fractions are converted into value-added products from the same SCB feedstock. The ethanol concentration obtained for the RS was comparable to values reported for alkaline-pretreated sugarcane bagasse in previous studies. For example, an ethanol concentration of 8.8 g L^{-1} was reported following NaOH pretreatment of SCB [55]. Higher ethanol concentrations of 11.0 and 26.1 g L^{-1} have also been achieved using sequential acid–alkaline pretreatment followed by pre-saccharification and simultaneous saccharification and fermentation (SSF), and steam explosion combined with alkaline pretreatment and optimized SSF, respectively [56,57]. Conversely, lower ethanol production has also been reported depending on the pretreatment strategy, hydrolysis efficiency, fermentation configuration, and the microorganism employed. For instance, an ethanol productivity of 0.3 g L^{-1} h^{-1} was obtained for NaOH-delignified SCB under SSF conditions [58]. Therefore, direct comparison among studies should be interpreted with caution, as bioethanol production from lignocellulosic biomass is strongly influenced by several factors, including the pretreatment strategy, hydrolysis and fermentation configuration, enzyme loading, substrate concentration, fermentation microorganism, and operating conditions.

From a broader perspective, the present study was designed as a laboratory-scale proof of concept investigation of an integrated biorefinery strategy for SCB valorization. The primary objective was not to provide a comprehensive characterization of the hydrolysate or detailed fermentation kinetics, but rather to evaluate whether the lignin-poor residue generated after AE could be further converted into bioethanol while simultaneously recovering lignin as a value-added product for subsequent lignin-based resin production. Although the hydrolysate was not chemically characterized in detail, the successful production of ethanol indicates that sufficient fermentable carbohydrates were available to support yeast fermentation under the investigated conditions. Therefore, the present results provide experimental evidence supporting the feasibility of the proposed sequential valorization strategy at the laboratory scale, in which lignin and carbohydrate fractions are successively converted into value-added products.

3.8. Characterization and Performance Evaluation of the E-Lign-Based Resin

The FTIR spectrum of the resin (Figure 7a) exhibits the main characteristic bands of modified lignin, confirming the successful synthesis of lignin-based resin. The strong band around 1624 cm^{-1} corresponds to conjugated C=O vibrations and aromatic ring vibrations, indicating that the lignin's aromatic structure is preserved after crosslinking. The broad band between 3400 and 3200 cm^{-1} is assigned to hydroxyl (–OH) groups, confirming the presence of reactive sites capable of forming hydrogen bonds and interacting with other molecules. This observation is consistent with previous studies, where OH groups attributed to methylol and phenolic hydroxyl groups were observed around 3324–3358 cm^{-1} [59]. Peaks observed around 1200–1000 cm^{-1} can be attributed to C–O vibrations and modifications induced by the crosslinking agents, suggesting the formation of covalent bridges between lignin chains and the crosslinker. Additionally, the presence of methylene bridges around 1379–1498 cm^{-1} further confirms the linkage between lignin and the crosslinking agent, indicating successful network formation [60].

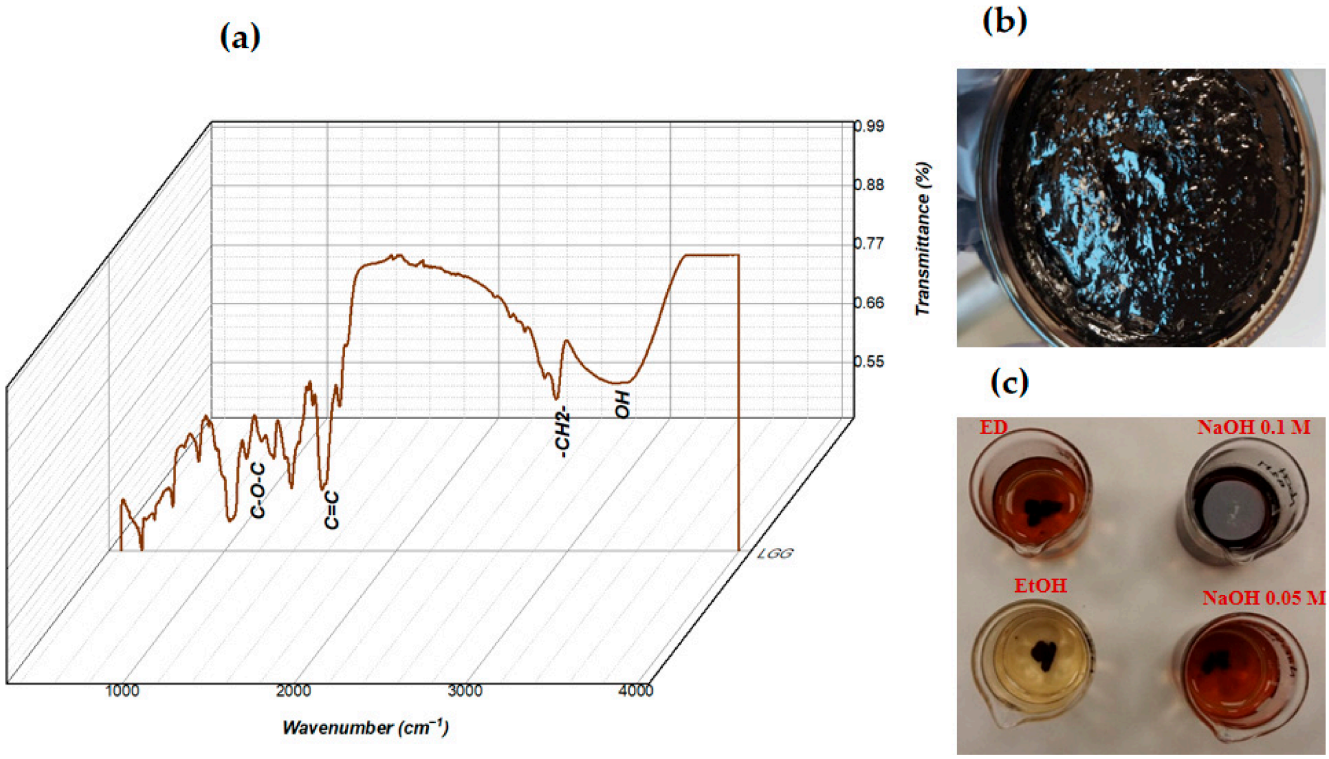


Figure 7. (**a**) FTIR spectrum of the lignin-based resin, (**b**) visual appearance of the synthesized resin, and (**c**) solubility of the resin in different solvents and alkaline solutions.

The visual appearance of the resin (Figure 7b) shows a homogeneous dark material, characteristic of crosslinked lignocellulosic resins, confirming successful synthesis. Solubility tests (Figure 7c) indicate that the resin is almost insoluble in water and ethanol, while showing partial solubility in dilute alkaline solutions (NaOH 0.05–0.1 M). This behavior is typical of crosslinked lignin-based resins, demonstrating the formation of a stable polymeric network while retaining accessible functional groups suitable for further applications, such as dye or heavy metal adsorption.

The importance of a crosslinked network in enhancing the performance of polymeric resins has been highlighted in other studies. For example, it has been reported that crosslinking improved the mechanical stability and environmental performance of epoxy resins, emphasizing that a well-developed polymeric network is critical for maintaining functionality in various applications [61].

In summary, the synthesized lignin-based resin maintains the aromatic structure of lignin, contains reactive hydroxyl groups, demonstrates effective crosslinking via glutaraldehyde/glyoxal, and exhibits solubility and stability characteristics suitable for environmental and industrial applications, consistent with the general advantages of crosslinked polymeric resins.

4. Conclusions

This study demonstrates the feasibility of an integrated valorization strategy for SCB through optimized AE of lignin followed by bioethanol production from the resulting lignin-poor residue. Using BBD, the effects of extraction temperature, NaOH concentration, solid-to-liquid ratio, and extraction time were systematically optimized to maximize lignin recovery and total phenolic content while preserving the carbohydrate-rich fraction for subsequent bioconversion. Under the optimized conditions, the proposed process enabled the efficient fractionation of SCB into two complementary streams suitable for downstream valorization.

Beyond lignin extraction, the recovered lignin was successfully incorporated as a partial substitute for petroleum-derived phenol in lignin-based resin formulations, demonstrating its potential as a renewable precursor for sustainable material applications. Furthermore, the lignin-poor residue generated after AE was successfully converted into bioethanol, confirming that lignin removal enhanced substrate accessibility while preserving sufficient fermentable carbohydrates for yeast fermentation. The higher ethanol production obtained from the RS compared with untreated SCB further supports the effectiveness of the proposed sequential processing strategy.

Collectively, these findings demonstrate that both the aromatic and carbohydrate fractions of SCB can be efficiently converted into value-added products within a single integrated process. The proposed approach therefore contributes to improving the overall utilization of lignocellulosic biomass while reducing waste generation and promoting a more sustainable biorefinery concept based on agricultural residues. As illustrated in Figure 8, the present work establishes a laboratory-scale proof of concept for an integrated biorefinery strategy in which recovered lignin is valorized for lignin-based resin production, while the lignin-poor residue is subsequently converted into bioethanol. Although the present study primarily demonstrates the experimental feasibility of this sequential valorization pathway, it establishes a solid foundation for future investigations involving comprehensive hydrolysate characterization, fermentation optimization, mass and energy balance analysis, process simulation, techno-economic assessment, and process scale-up. Overall, the proposed strategy provides a promising framework for the sustainable and integrated utilization of SCB within a circular bioeconomy.

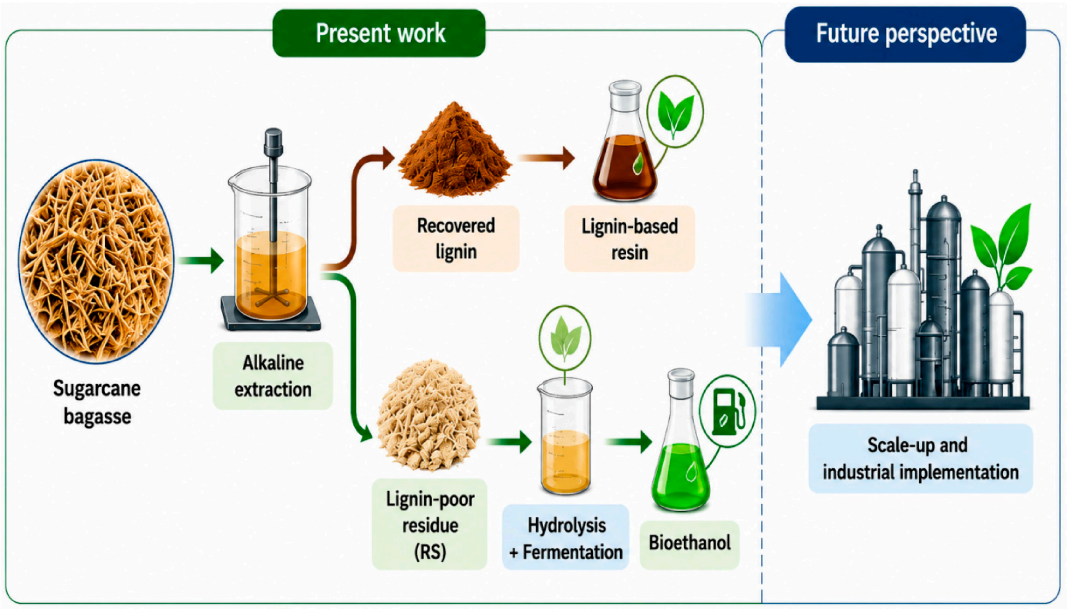


Figure 8. Schematic overview of the integrated valorization strategy proposed in this study, illustrating lignin recovery, lignin-based resin production, bioethanol generation from the lignin-poor residue, and the future perspective toward industrial implementation.

Author Contributions: Conceptualization, H.E. and D.E.; methodology, H.E., D.E. and A.O.; software, H.E.; validation, D.E., Z.E.A., A.O. and K.L.; formal analysis, H.E. and A.O.; investigation, D.E. and Z.E.A.; resources, D.E., Z.E.A. and K.L.; data curation, H.E. and D.E.; writing—original draft preparation, H.E. and D.E.; writing—review and editing, D.E., Z.E.A., A.O. and Z.E.A.; visualization, H.E. and D.E.; supervision, D.E., Z.E.A. and K.L.; project administration, D.E., Z.E.A. and K.L.; funding acquisition. All authors have read and agreed to the published version of the manuscript.

Funding: This research received no external funding.

Institutional Review Board Statement: Not applicable.

Informed Consent Statement: Not applicable.

Data Availability Statement: The original contributions presented in this study are included in the article. Further inquiries can be directed to the corresponding author.

Acknowledgments: The authors would like to express their sincere gratitude to UM6P for providing the necessary facilities and support throughout this study. We also acknowledge the valuable guidance and technical assistance provided by AgBS and CBS laboratories. We edited the output and take full responsibility for the content of this publication. During the preparation of this manuscript, ChatGPT (GPT-5.5-mini, OpenAI) was used to assist in refining technical phrasing and grammar.

Conflicts of Interest: The authors declare no conflicts of interest.

Abbreviations

The following abbreviations are used in this manuscript:

SCB	Sugarcane Bagasse
BBD	Box–Behnken Design
TPC	Total Phenolic Content
PLC	Pure Lignin Content
GAE	Gallic Acid Equivalent
FTIR	Fourier Transform Infrared Spectroscopy

TGA	Thermogravimetric Analysis
AE	Alkaline Extraction
RSM	Response Surface Methodology
E-Lign	Extracted Lignin
NREL	National Renewable Energy Laboratory
ADF	Acid Detergent Fiber
RS	Residual Solid
UT-SCB	Untreated Sugarcane Bagasse
LFAF	Lignin-Free Acidic Filtrate
GC-MS	Gas Chromatography–Mass Spectrometry
ANOVA	Analysis of Variance

References

1. Raza, Q.-U.-A.; Bashir, M.A.; Rehim, A.; Sial, M.U.; Ali Raza, H.M.; Atif, H.M.; Brito, A.F.; Geng, Y. Sugarcane industrial byproducts as challenges to environmental safety and their remedies: A review. *Water* **2021**, *13*, 3495. [CrossRef]
2. Oulkhir, A.; Lyamlouli, K.; Elfahmy, H.; Benmansour, M.R.; Tayibi, S.; Elalami, D.; Taarji, N.; Etahiri, A.; Benhida, R. Remarkable Effect of Sugar Waste Pyrolysis Oil as a Calcite Collector for Enhanced Phosphate Beneficiation via Reverse Flotation. *ACS Sustain. Chem. Eng.* **2025**, *13*, 6706–6719. [CrossRef]
3. Meghana; Shastri, Y. Sustainable valorization of sugar industry waste: Status, opportunities, and challenges. *Bioresour. Technol.* **2020**, *303*, 122929. [CrossRef]
4. Alokika; Anu; Kumar, A.; Kumar, V.; Singh, B. Cellulosic and hemicellulosic fractions of sugarcane bagasse: Potential, challenges, and future perspective. *Int. J. Biol. Macromol.* **2021**, *169*, 564–582. [CrossRef]
5. Oulkhir, A.; Lyamlouli, K.; Danouche, M.; Benhida, R. Biosorption of a Cationic Dye Using Raw and Functionalized *Chenopodium quinoa* Pericarp Biomass after Saponin Glycosides Extraction. *J. Environ. Chem. Eng.* **2023**, *11*, 110419. [CrossRef]
6. Scelsi, E.; Angelini, A.; Pastore, C. Deep eutectic solvents for the valorisation of lignocellulosic biomasses towards fine chemicals. *Biomass* **2021**, *1*, 29–59. [CrossRef]
7. Oulkhir, A.; Segmami, A.; Ou-Douaou, A.; Etahiri, A.; Ait Benhamou, A.; Lyamlouli, K.; Benhida, R. Lignin-Based Flotation Reagents for Sustainable Mineral Processing. *Prog. Mater. Sci.* **2026**, *160*, 101679. [CrossRef]
8. Morales, A.; Gullón, B.; Dávila, I.; Eibes, G.; Labidi, J.; Gullón, P. Optimization of alkaline pretreatment for the co-production of biopolymer lignin and bioethanol from chestnut shells following a biorefinery approach. *Ind. Crops Prod.* **2018**, *124*, 582–592. [CrossRef]
9. Ang, A.F.; Ashari, Z.; Lee, S.H.; Md Tahir, P.; Halis, R. Lignin-based copolymer adhesives for composite wood panels—A review. *Int. J. Adhes. Adhes.* **2019**, *95*, 102408. [CrossRef]
10. Kerrou, M.; Bouslamti, N.; Raada, A.; Elanssari, A.; Mrani, D.; Slimani, M.S. The use of sugarcane bagasse to remove the organic dyes from wastewater. *Int. J. Anal. Chem.* **2021**, *2021*, 5570806. [CrossRef] [PubMed]
11. Zielińska, M.; Bułkowska, K. Agricultural wastes and their by-products for the energy market. *Energies* **2024**, *17*, 2099. [CrossRef]
12. Barciela, P.; Pérez-Vázquez, A.; Fraga-Corral, M.; Prieto, M.A. Utility Aspects of Sugarcane Bagasse as a Feedstock for Bioethanol Production: Leading Role of Steam Explosion as a Pretreatment Technique. *Processes* **2023**, *11*, 3116. [CrossRef]
13. Antunes, F.; Mota, I.F.; Burgal Jda, S.; Pintado, M.; Santos Costa, P. A review on the valorization of lignin from sugarcane by-products: From extraction to application. *Biomass Bioenergy* **2022**, *166*, 106603. [CrossRef]
14. Galbe, M.; Wallberg, O. Pretreatment for biorefineries: A review of common methods for efficient utilisation of lignocellulosic materials. *Biotechnol. Biofuels Bioprod.* **2019**, *12*, 294. [CrossRef] [PubMed]
15. Devi, A.; Bajar, S.; Kour, H.; Kothari, R. Lignocellulosic biomass valorization for bioethanol production: A circular bioeconomy approach. *BioEnergy Res.* **2022**, *15*, 1820–1841. [CrossRef] [PubMed]
16. Houghton, T.P.; Stevens, D.M.; Pryfogle, P.A.; Wright, C.T.; Radtke, C.W. The effect of drying temperature on the composition of biomass. *Appl. Biochem. Biotechnol.* **2009**, *153*, 4–10. [CrossRef] [PubMed]
17. Mokobia, E.K.; Christopher, M. Proximate analyses of selected biomass material. *Int. J. Res. Publ. Rev.* **2022**, *3*, 778–783.
18. Yulia, R.; Husin, H.; Zaki, M.; Razali, N.; Nasution, F.; Ahmadi, A.; Sy, Y.; Syafiie, S. Enhancing sustainability through optimized adsorption using a novel Klason-lignin-based biosorbent derived from sugar-palm fruit shells for efficient removal of Pb(II) and Cd(II). *Energy Nexus* **2025**, *17*, 100398. [CrossRef]
19. Tibin, M.A.M.; Ibrahim, B.M.M.; Abdalla, S.E.M.; Abutaba, Y.I.M.; Jadalla, J.B.; Ebrahiem, M.A. Chemical composition and in vitro digestibility of some range plants. *Open J. Plant Sci.* **2021**, *6*, 94–98. [CrossRef]
20. Luaces, P.; Pascual, M.; Pérez, A.G.; Sanz, C. An easy-to-use procedure for the measurement of total phenolic compounds in olive fruit. *Antioxidants* **2021**, *10*, 1656. [CrossRef] [PubMed]

21. US Environmental Protection Agency. *Performance Specification 15—Performance Specification for Extractive FTIR Continuous Emissions Monitor Systems in Stationary Sources*; U.S. Environmental Protection Agency: Washington, DC, USA, 2019.
22. Farrokh, N.T.; Suopajärvi, H.; Sulasalmi, P.; Fabritius, T. A thermogravimetric analysis of lignin char combustion. *Energy Procedia* **2019**, *158*, 1241–1248. [CrossRef]
23. Jahanbakhshi, A.; Salehi, R. Processing watermelon waste using *Saccharomyces cerevisiae* yeast and the fermentation method for bioethanol production. *J. Food Process Eng.* **2019**, *42*, e13283. [CrossRef]
24. Siahkamari, M.; Emmanuel, S.; Hodge, D.B.; Nejad, M. Lignin-glyoxal: A fully biobased formaldehyde-free wood adhesive for interior engineered wood products. *ACS Sustain. Chem. Eng.* **2022**, *10*, 3430–3441. [CrossRef]
25. Boer, F.D.; Valette, J.; Commandré, J.-M.; Fournier, M.; Thévenon, M.-F. Slow pyrolysis of sugarcane bagasse for the production of char and the potential of its by-product for wood protection. *J. Renew. Mater.* **2021**, *9*, 98–116. [CrossRef]
26. Nasution, M.H.; Lelinasari, S.; Kelana, M.G.S. A review of sugarcane bagasse pretreatment for bioethanol production. *IOP Conf. Ser. Earth Environ. Sci.* **2022**, *963*, 012014. [CrossRef]
27. Tran, P.H.N.; Ko, J.K.; Gong, G.; Um, Y.; Lee, S.-M. Improved simultaneous co-fermentation of glucose and xylose by *Saccharomyces cerevisiae* for efficient lignocellulosic biorefinery. *Biotechnol. Biofuels* **2020**, *13*, 12. [CrossRef] [PubMed]
28. Shabbirahmed, A.M.; Haldar, D.; Dey, P.; Patel, A.K.; Singhania, R.R.; Dong, C.-D.; Purkait, M.K. Sugarcane bagasse into value-added products: A review. *Environ. Sci. Pollut. Res.* **2022**, *29*, 62785–62806. [CrossRef] [PubMed]
29. Wahba, S.M.R.; Darwish, A.S.; Shehata, I.H.; Abd Elhalem, S.S. Sugarcane bagasse lignin, and silica gel and magneto-silica as drug vehicles for development of innocuous methotrexate drug against rheumatoid arthritis disease in albino rats. *Mater. Sci. Eng. C* **2015**, *48*, 599–610. [CrossRef] [PubMed]
30. Costa, E.S.; Perlatti, B.; da Silva, E.M.; Matos, A.P.; da Silva, M.F.G.F.; Fernandes, J.B.; Zuin, V.G.; da Silva, C.M.P.; Forim, M.R. Use of lignins from sugarcane bagasse for assembling microparticles loaded with Azadirachta indica extracts for use as neem-based organic insecticides. *J. Braz. Chem. Soc.* **2017**, *28*, 126–135. [CrossRef]
31. Suriyachai, N.; Champreda, V.; Kraikul, N.; Techanan, W.; Laosiripojana, N. Fractionation of lignocellulosic biopolymers from sugarcane bagasse using formic acid-catalyzed organosolv process. *3 Biotech* **2018**, *8*, 221. [CrossRef] [PubMed]
32. Ji, Q.; Yu, X.; Wu, P.; Yagoub, A.E.A.; Chen, L.; Mustapha, A.T.; Zhou, C. Pretreatment of sugarcane bagasse with deep eutectic solvents affect the structure and morphology of lignin. *Ind. Crops Prod.* **2021**, *173*, 114108. [CrossRef]
33. Mota, I.F.; da Silva Burgal, J.; Antunes, F.; Pintado, M.E.; Costa, P.S. High value-added lignin extracts from sugarcane by-products. *Int. J. Biol. Macromol.* **2023**, *230*, 123144. [CrossRef] [PubMed]
34. Morán-Aguilar, M.G.; Calderón-Santoyo, M.; de Souza Oliveira, R.P.; Aguilar-Uscanga, M.G.; Domínguez, J.M. Deconstructing sugarcane bagasse lignocellulose by acid-based deep eutectic solvents to enhance enzymatic digestibility. *Carbohydr. Polym.* **2022**, *292*, 120097. [CrossRef] [PubMed]
35. Lam, H.Q.; Le Bigot, Y.; Delmas, M.; Avignon, G. A new procedure for the destructuring of vegetable matter at atmospheric pressure by a catalyst/solvant system of formic acid/acetic acid. Applied to the pulping of triticale straw. *Ind. Crops Prod.* **2001**, *14*, 139–144. [CrossRef]
36. Wang, N.; Xu, B.; Wang, X.; Lang, J.; Zhang, H. Chemical and Structural Elucidation of Lignin and Cellulose Isolated Using DES from Bagasse Based on Alkaline and Hydrothermal Pretreatment. *Polymers* **2022**, *14*, 2756. [CrossRef] [PubMed]
37. Yemis, O.; Mazza, G. Optimization of furfural and HMF production from wheat straw by a microwave-assisted process. *Bioresour. Technol.* **2012**, *109*, 215–223. [CrossRef] [PubMed]
38. Xin, C.Y.; Zulkornain, A.S.; Ya'akob, H.; Puzic, S.M.; Wan Azelee, N.I. Effect of alkaline concentration on lignin extraction from sugarcane bagasse. *Bioprocess Biomass Technol.* **2024**, *3*, 13–19. [CrossRef]
39. Ratanasumarn, N.; Chitprasert, P. Optimization of lignin extraction from sugarcane bagasse for cosmetic applications. *Int. J. Biol. Macromol.* **2020**, *153*, 138–145. [CrossRef] [PubMed]
40. Yan, P.; Xu, Z.; Zhang, C.; Liu, X.; Xu, W.; Zhang, Z.C. Fractionation of lignin from eucalyptus bark using amine-sulfonate functionalized ionic liquids. *Green Chem.* **2015**, *17*, 4700–4710. [CrossRef]
41. Vo, H.T.; Kim, C.S.; Lee, S.D.; Lee, H. Ionic liquid-assisted separation of carbohydrates from Lignocellulosic Biomass. *Bull. Korean Chem. Soc.* **2016**, *37*, 1305–1312. [CrossRef]
42. Cherif, M.F.; Trache, D.; Brosse, N.; Benaliouche, F.; Tarchoun, A.F. Comparison of the Physicochemical Properties and Thermal Stability of Organosolv and Kraft Lignins from Hardwood and Softwood Biomass for Their Potential Valorization. *Waste Biomass Valor.* **2020**, *11*, 6541–6553. [CrossRef]
43. Zhang, Q.; Li, H.; Guo, Z.; Xu, F. High Purity and Low Molecular Weight Lignin Nano-Particles Extracted from Acid-Assisted MIBK Pretreatment. *Polymers* **2020**, *12*, 378. [CrossRef] [PubMed]
44. Dhara, S.; Samanta, N.S.; Uppaluri, R.; Purkait, M.K. High-purity alkaline lignine extraction from *Saccharum ravannae* and optimization of lignin recovery through response surface methodology. *Int. J. Biol. Macromol.* **2023**, *234*, 123594. [CrossRef] [PubMed]

45. Romaní, A.; Ruiz, H.A.; Teixeira, J.A.; Domingues, L. Valorization of Eucalyptus wood by glycerol-organosolv pretreatment within the biorefinery concept: An integrated and intensified approach. *Renew. Energy* **2016**, *95*, 1–9. [CrossRef]
46. Sunar, S.L.; Oruganti, R.K.; Bhattacharyya, D.; Shee, D.; Panda, T.K. Pretreatment of sugarcane bagasse using ionic liquid for enhanced enzymatic saccharification and lignin recovery: Process optimization by response surface methodology. *Cellulose* **2024**, *31*, 2151–2173. [CrossRef]
47. Aridia, A.S.; Ling, C.N.; Ishak, N.A.; Yusof, N.N.M.; Ahmed, M.F.M.; Yusof, Y.A. Structural FTIR analysis of cellulose functional groups isolated from Leucaena leucocephala pods using diffferent bleaching agents. *AgriRxiv* **2020**, *2020*, 20203561010. [CrossRef]
48. Balasubramanian, P.; Ramalingam, S.; Abu Javid, M.; Raghava Rao, J. Lignin Based Colorant: Modified Black Liquor for Leather Surface Coating Application. *JALCA* **2018**, *113*, 311–317.
49. Elshafie, M.; Taha, M.G.; Elhamamsy, S.M.; Moustafa, Y.; Elazab, W.I.M. Thermal analysis of the prepared lignin/graphene oxide/polyurethane composite. *Egypt. J. Pet.* **2020**, *29*, 195–201. [CrossRef]
50. Pe, J.A.; Mun, J.S.; Mun, S.P. Thermal characterization of kraft lignin prepared from mixed hardwoods. *BioResources* **2023**, *18*, 926–936.
51. Ramezani, N.; Sain, M. Thermal and Physiochemical Characterization of Lignin Extracted from Wheat Straw by Organosolv Process. *J. Polym. Environ.* **2018**, *26*, 3109–3116. [CrossRef]
52. Brebu, M.; Ioniță, D.; Stoleru, E. Thermal behavior and conversion of agriculture biomass residues by torrefaction and pyrolysis. *Sci. Rep.* **2025**, *15*, 11505. [CrossRef] [PubMed]
53. Limami, A.M.; Glévarec, G.; Ricoult, C.; Cliquet, J.-B.; Planchet, E. Concerted modulation of alanine and glutamate metabolism in young Medicago truncatula seedlings under hypoxic stress. *J. Exp. Bot.* **2008**, *59*, 2325–2335. [CrossRef] [PubMed]
54. Zhou, Z.; Cheng, Y.; Zhang, W.; Jiang, J.; Lei, F. Characterization of lignin from sugarcane bagasse pretreated with green liquor combined with ethanol and hydrogen peroxide. *Bioresources* **2016**, *11*, 3191–3203. [CrossRef]
55. Carvalho, D.M.; de Queiroz, J.H.; Colodette, J.L. Assessment of alkaline pretreatment for the production of bioethanol from eucalyptus, sugarcane bagasse and sugarcane straw. *Ind. Crops Prod.* **2016**, *94*, 932–941. [CrossRef]
56. Banoth, C.; Sunkar, B.; Tondamanati, P.R.; Bhukya, B. Improved physicochemical pretreatment and enzymatic hydrolysis of rice straw for bioethanol production by yeast fermentation. *3 Biotech* **2017**, *7*, 334. [CrossRef] [PubMed]
57. de Souza, C.J.A.; Costa, D.A.; Rodrigues, M.Q.R.B.; Santos, A.F.; Lopes, M.R.; Abrantes, A.B.P.; Costa, P.d.S.; Silveira, W.B.; Passos, F.M.L.; Fietto, L.G. The influence of presaccharification, fermentation temperature and yeast strain on ethanol production from sugarcane bagasse. *Bioresour. Technol.* **2012**, *109*, 63–69. [CrossRef] [PubMed]
58. Santos, J.R.A.; Souto-Maior, A.M.; Gouveia, E.R. Comparison of SHF and SSF processes from sugar cane bagasse for ethanol production by *Saccharomyces cerevisiae*. *Quím. Nova* **2010**, *33*, 904–908. [CrossRef]
59. Yaakob, M.N.A.; Roslan, R.; Salim, N.; Mustapha, S.N.H. Structural and thermal behavior of lignin-based formaldehyde-free phenolic resin. *Mater. Today Proc.* **2022**, *51*, 1388–1391. [CrossRef]
60. Galdino, D.S.; Kondo, M.Y.; De Araujo, V.A.; Ferrufino, G.L.A.A.; Faustino, E.; dos Santos, H.F.; Christoforo, A.L.; Luna, C.M.R.; de Campos, C.I. Thermal and Gluing Properties of Phenol-Based Resin with Lignin for Potential Application in Structural Composites. *Polymers* **2023**, *15*, 357. [CrossRef] [PubMed]
61. Abd-Alkhaleq, W.A.A.; Ismael, M.Q. Enhancing the Moisture resistance in Asphalt Mixtures Using Epoxy Resin. *Eng. Technol. Appl. Sci. Res.* **2025**, *15*, 26868–26873. [CrossRef]

Disclaimer/Publisher's Note: The statements, opinions and data contained in all publications are solely those of the individual author(s) and contributor(s) and not of MDPI and/or the editor(s). MDPI and/or the editor(s) disclaim responsibility for any injury to people or property resulting from any ideas, methods, instructions or products referred to in the content.